Eur Biophys J (2000) 29: 523–534
DOI 10.1007/s002490000106

ARTICLE

Yu Zhou Tang · Wei Zu Chen · Cun Xin Wang

Molecular dynamics simulations of the gramicidin A-dimyristoylphosphatidylcholine system with an ion in the channel pore region

Received: 27 June 2000 / Revised version: 31 August 2000 / Accepted: 31 August 2000 / Published online: 24 October 2000

Abstract To investigate the process of ion permeation in an ion channel systematically, we performed molecular dynamics (MD) simulations on a gramicidin A (GA)-phospholipid model system with an ion in the channel pore region. Each of the three types of ions (Ca^{2+}, Na^{+}, Cl^{-}) was placed at five different positions along the channel axis by replacing a water molecule. MD simulations were performed on each system at constant pressure and constant temperature. The MD trajectories showed that the Ca^{2+} and Na^{+} ions could stably fluctuate in the pore region, but the Cl^{-} ion was pushed out because of the unfavorable interaction with the channel. This result is consistent with experimental data. It was also found that the conformation of the GA channel underwent a significant change due to the presence of the ion, and the two ends of the GA monomer were more flexible than its middle region. In particular, the dramatic change of local pore radius near the ion indicated this kind of deformation. The strong interaction between the ion and carbonyl oxygen atoms of GA was the major contributor to this change. Furthermore, it was found that the ethanolamine group of the GA molecule was the most flexible group in the GA channel and often observed to block the entrance of GA. These results imply that the deformation of channel structure plays a very important factor in ion permeation, and the ethanolamine group may play a key role in regulating ion entry into the pore. In conclusion, our results indicate that the ion has a dominant influence on the structure of the GA channel and that the flexibility of the ion channel is a crucial factor in the ion permeation process.

Key words Gramicidin A · Dimyristoylphosphatidylcholine · Ion channel · Ion-protein interactions · Computer modeling

Y. Z. Tang[1] (✉) · W. Z. Chen · C. X. Wang
Center for Biomedical Engineering,
Beijing Polytechnic University,
Beijing 100022, P.R. China
E-mail: cxwang@bjpu.edu.cn

Y. Z. Tang
Department of Astronomy and Applied Physics,
University of Science and Technology of China,
Hefei 230026, P.R. China

Present address:
[1]Biophysics and Computational Biology Program,
University of Illinois at Urbana-Champaign,
Urbana, IL 61801, USA

Introduction

An ion channel is one of the most important proteins that exist in a biological membrane. By allowing selective and regulated diffusion of ions across the lipid bilayer membrane, ion channels play a key role in many important physiological processes, ranging from signal transmission to muscle contraction (Latorre 1986). Hundreds of functionally different ion channels have been identified and their amino acid sequences have been obtained. A dominant characteristic of ion channels is that they form an aqueous pore that helps ions traverse the channel (Montal 1996). However, in sharp contrast to the wealth of sequence information, structural information of ion channels at atomic resolution is very limited owing to difficulty in purification and obtaining crystals of membrane proteins (Montal 1996). Therefore, despite much progress made in this field, it is still a challenge for researchers to explore functional mechanisms of ion channels at the molecular level.

MD simulation methods can provide us with a wealth of information on the structural and dynamic properties of macromolecules at the atomic level. With the rapid development of computer power, the molecular dynamics (MD) simulation approach is used more and more as a valid tool for many studies of biomolecules. However, owing to the complexity of biological membranes and the limitation of computational power, it was not until the end of the 1980s that MD simulation was extended to studies of biological membrane systems,

including lipid bilayers and membrane proteins. In the following 10 years, a large number of MD simulation studies in this field have been reported (Pastor 1994; Jakobsson 1997; Merz 1997). Although there still exist some problems in this field, many successful simulations with different ensembles (NVT, NPT, NPnγT) and different force fields (GROMOS, AMBER, CHARMM) have been performed and validated (Berger et al. 1997). These successes indicate that different force field and technical aspects of MD simulation, which were formerly used for simulations of proteins and nucleic acids, can successfully be applied to the study of biological membrane systems. The refinement of methodologies will continue, but the "proof-of-concept" is done (Jakobsson 1997).

Gramicidin A (GA), a linear antibiotic pentadecapeptide, can form a voltage-gated ion channel in a membrane as a head-to-head dimer of two single-stranded right-handed helices (Wallace 1990). Owing to its small size and exceptionally well-defined structure and function, GA has been studied widely as a model for ion channels and lipid-protein interactions by both experimental and theoretical methods in the past 20 years (Andersen 1984; Wallace 1990; Roux and Karplus 1994; Koeppe and Andersen 1996). In particular, it was used as the typical model for MD simulation of an ion channel (Roux and Karplus 1994). Theoretical studies of the gramicidin channel at the atomic level started in 1973 with the simplified dipole model developed by Fischer et al. (1981); subsequently, ion transportation in the GA channel was first investigated by Pullman (1985). However, because of the limitation on computational power and lack of high-resolution structure in a membrane environment, the oldest model of GA was simplified with a stylized periodic helix. Later, more complex and realistic models were proposed, in which the channel flexibility (Mackay et al. 1984), the conformation of the side chains (Fornili et al. 1984), and the simplified treatment of the membrane (Roux and Karplus 1988; Chiu et al. 1989) were taken into account. In the past four years, MD simulation methods of the GA channel have evolved to a new stage and an explicit lipid bilayer environment was introduced into the model system (Woolf and Roux 1994, 1996; Chiu et al. 1999a, b).

Experimental work has indicated that only monovalent cations (Na^+, K^+, Cs^+) can permeate the GA channel, while a divalent cation (Ca^{2+}) will block the ion conductance of the GA channel and an anion (Cl^-) cannot enter into the channel pore region at all (Andersen 1984; Wallace 1990). The main goal of the present work is to explore the fundamental principles of ion-protein interactions and to help us acquire a better understanding of the ion permeation process in the channel. In our previous study (Tang et al. 1999), we proposed a new method to construct a suitable initial configuration for the GA-DMPC (dimyristoylphosphatidylcholine) model system. The present work is an extension of our previous work by introducing ions into the GA-DMPC system. Three types of ions (Na^+, Ca^{2+}, Cl^-) were placed in the pore region of the GA channel, and MD simulations were performed for the model system without any artificial constraint. Although similar MD simulations of this model system have been done in previous studies (Woolf and Roux 1996, 1997; Chiu et al. 1999a, b), a different simulation boundary condition (NPT) and force field (GROMOS 96) were used in this work. In addition, as detailed later, the simulation procedure and the analysis method were also somewhat different from previous work.

The following is an outline of our report. The method for building up the model system and the computational details are presented in the next section. Then, we report the analysis results in detail, such as the dynamic properties of ions and water molecules in the channel pore region, the average structural properties of the GA channel in different models, the interaction energies between different components of the model system, and our explanations for these results. Finally, some important points are summarized in the conclusion.

Methodology

Each simulation system contained a GA dimer, 16 DMPC lipids, and 1050 water molecules (4252 atoms in total). The three-dimensional structure of GA, determined by solid-state NMR experiments (Ketchem et al. 1993), was used as the initial structure since the NMR structure was determined in a lipid bilayer. The initial structure of DMPC was selected from a library of equilibrated DMPC configurations obtained from previous MD simulations of the GA-DMPC system (Egberts et al. 1994; Tang et al. 1999). In order to get a reasonable starting configuration for this model, we used a special method described in detail in our previous paper (Tang et al. 1999).

With the initial configuration setup, 100 ps MD simulation divided into four runs was used to equilibrate the system. First, 20 ps MD simulation was performed at constant pressure and constant temperature. Harmonic restraints were added to all the GA atoms and the DMPC phosphorus atoms with respect to their initial positions. Then, the system was subjected to 30 ps MD simulation using the simulated annealing (SA) method (Kirkpatrick et al. 1983). The system was simulated at 500 K in the first 10 ps and then cooled from 500 K to 340 K at a rate of 8 K/ps during the following 20 ps. The phosphorus atoms of DMPC were restrained with a reduced force constant during this stage to let DMPC maintain the bilayer form but also provide enough flexibility for DMPC molecules. In addition, the hydrogen bonds (H-bonds) that were formed by the backbone atoms of GA were restrained in order to ensure that the conformation of GA was not destroyed at the high temperature. Further, 50 ps simulation was used again to the equilibrate system at normal temperature, during which the restraints on the phosphorus atoms of DMPC were removed and the restraints on the H-bonds were gradually decreased and completely removed during the last 30 ps simulation.

Once the equilibrated system was prepared, more simulations were performed on the system in the following two ways:

1. 100 ps MD simulation was performed continuously for the same system and the trajectory data were recorded. These MD data were used to compare with other systems in which an ion was put in the GA pore region.
2. As shown in Fig. 1, each of three types of ions (Na^+, Ca^{2+}, and Cl^-) were put at the five positions in the GA pore region by replacing one of five water molecules, which were designated as P1–P5 in Fig. 1. Owing to the symmetry of the GA dimer, all

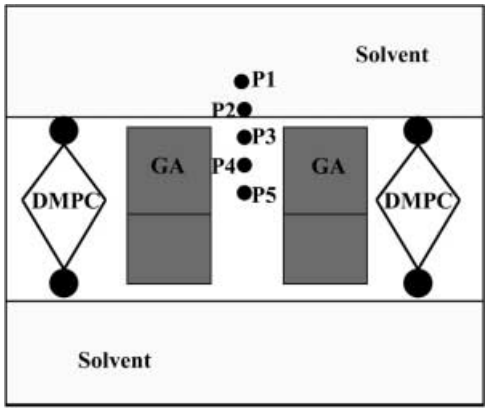

Fig. 1 Schematic view of the GA-DMPC model system. The ions in the pore region were located at five positions designated as *P1*, *P2*, *P3*, *P4*, and *P5* in the figure

these substitutions were accomplished in the one GA monomer. It appeared that there was only single ion occupancy in each GA-DMPC model. In order to distinguish the different models, they were designated by the ion type and the position of the ion. For example, the CA-P1 model means that the model has the Ca^{2+} ion located at the P1 position. The model without the ion was designated as GD-H2O for comparison with the 15 model systems with ions. In order to let the systems with ions have enough time to respond to the presence of the ion, the GA-DMPC systems with ions were equilibrated again with position restraint on the ion at each chosen position, followed by MD without the restraint. The MD simulations for each system consisted of 50 ps equilibration followed by 50 ps data collection.

All EM and MD simulations in the present work were performed using the GROMOS 96 package (van Gunsteren et al. 1996). Standard parameters of the GROMOS 96 force field were used for GA. For DMPC, we set up a set of parameters according to previous work (Egberts et al. 1994; Tang et al. 1999). The united atom model was used for the parameters, in which non-polar hydrogen atoms were included in the carbon atoms while polar hydrogen atoms were treated explicitly. The Ryckaert-Bellemans potential (Ryckaert and Bellemans 1975) was used for the dihedral angles of the alkyl chains of DMPC, such as the dihedral angles of CH_2-CH_2-CH_2-CH_2 and CH_2-CH_2-CH_2-CH_3, because this potential was demonstrated to be very suitable for the MD simulation of lipid bilayers (Egberts and Berendsen 1988; Pastor et al. 1991). The SPC/E model was used for water molecules (Berendsen et al. 1987). The bond lengths were constrained by the SHAKE algorithm (Ryckaert et al. 1977; van Gunsteren and Berendsen 1977) in all simulations. The 0.8 nm cut-off radius was applied for short-range interactions and 1.4 nm for long-range interactions using the twin-range method. Since the model systems in the present study contained charged particles, ions, and strongly polar groups, such as the head-groups of the DMPC lipid, it was very important to deal with electrostatic interactions carefully in MD simulations. Therefore, reaction-field calculations have been incorporated in all the simulations since the inclusion of the reaction field has a significant improvement on the calculation for the long-range electrostatic interaction (Hunenberger and van Gunsteren 1998). Periodic boundary conditions were applied along all three dimensions and all MD simulations were performed at constant temperature and constant pressure by weak coupling to a temperature bath and a pressure bath (Berendsen et al. 1984). Except during the SA process, the model system in all MD simulations was kept at 340 K, above the transition temperature of DMPC lipid from the gel phase to the liquid crystal phase. In addition, there has been considerable debate on the usage of normal pressure (NTP ensemble) or surface tension ($NP_n\gamma T$ ensemble) as the boundary condition in computer simulations of membrane systems (Jakobsson 1997; Merz 1997). Recent studies have demonstrated that little practical difference was seen in simulations with NTP and $NP_n\gamma T$ ensembles (Tieleman and Berendsen 1996); therefore, we chose the NTP ensemble for our work. The MD time step was set to 2 fs, and trajectory data were collected every 50 steps (0.1 ps).

In the analysis of simulation results, pore radius was measured using the PORE program (Cheng et al. 1998), which was developed from the HOLE program (Smart et al. 1993) and was used to generate a pore radius as a function of distance along the pore axis. Graphic display and examination of models were carried out with Rasmol (Sayle and Millner-White 1995) and MSI Insight II software (Molecular Simulations, San Diego, Calif.).

Results and discussion

Validity of construction method and simulation quality

Although there are many reports on MD simulations of lipid bilayer and membrane-protein systems, there is still a lack of effective and fast methods to construct an initial configuration for such a system. However, a reasonable initial configuration is very important for MD simulations of membrane systems owing to the slow relaxation time of the membrane (Pastor 1994; Woolf and Roux 1996). In particular, a correct choice of surface area for the membrane system plays a key issue in constructing a suitable initial configuration, since overestimate or underestimate of this value will cause the system to deviate from the expectant state within the hundreds of picoseconds simulation time (Heller et al. 1993). However, it is difficult to choose this value exactly using recent experimental tools. For instance, a wide range from 0.52 to 0.74 nm^2 was reported for the surface area per DMPC lipid (Woolf and Roux 1996). Therefore, much care should be paid to this issue when MD simulation is performed for a membrane system. In our previous work, a special construction method was proposed and validated for the GA-DMPC system (Tang et al. 1999). In the present work, a SA procedure was added to the equilibration process to improve our construction method.

To examine the influence of the SA process in our method, the change in surface area for the GD-H2O system with simulation time is showed in Fig. 2, where the period from 10 to 50 ps is the SA process. The surface area increased from 8.53 to 9.45 nm^2 during the first 20 ps (from 10 to 30 ps) because the system was heated at high temperature (500 K). Then, the area decreased rapidly as the system was cooled from 500 to 340 K within the 20 ps (from 30 to 50 ps). With further 70 ps simulation, the surface area converged to 8.05 nm^2, which is similar to the initial value for the system (7.99 nm^2). This shows that the model system was not trapped in a local minimum by our method. On the other hand, Table 1 lists the simulation results, including average surface area, average volume, and average potential energy of the system, over the last 50 ps equilibrated simulation for the 15 model systems with ions.

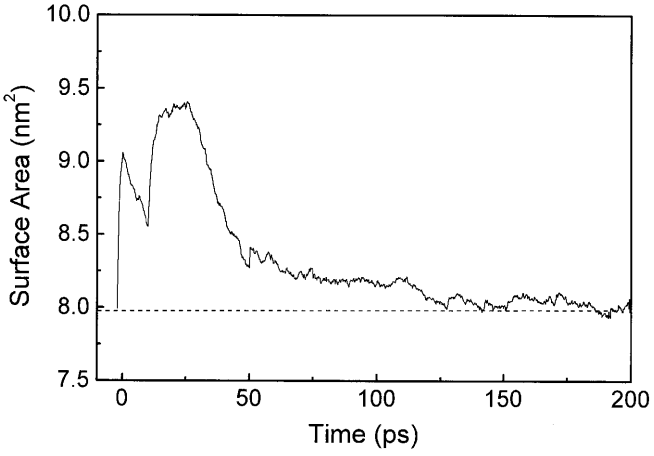

Fig. 2 Change in surface area with simulation time for the GD-H2O model system. All the 200 ps simulation, including the 100 ps equilibration process, is shown in the figure. It is found that the surface area of the system is equilibrated well after the 100 ps equilibration process

Table 1 Convergence behavior of MD simulations for different models

System	Surface area (nm^2)	Volume (nm^3)	Potential energy (kJ/mol)
NA-P1	7.95	54.8 ± 0.2	-53300 ± 200
NA-P2	7.98	55.2 ± 0.2	-53200 ± 190
NA-P3	8.01	55.1 ± 0.2	-53130 ± 200
NA-P4	8.09	55.1 ± 0.2	-53110 ± 200
NA-P5	8.13	55.0 ± 0.2	-53110 ± 190
CA-P1	7.90	55.1 ± 0.2	-54030 ± 190
CA-P2[a]	7.98	55.1 ± 0.2	-53940 ± 200
CA-P3	7.87	55.2 ± 0.2	-53820 ± 180
CA-P4	8.07	55.0 ± 0.2	-53740 ± 180
CA-P5	8.01	55.0 ± 0.2	-53710 ± 210
CL-P1	7.98	55.2 ± 0.2	-53190 ± 200
CL-P2	8.17	55.0 ± 0.1	-53070 ± 200
CL-P3	8.07	55.1 ± 0.2	-53160 ± 210
CL-P4	8.09	55.2 ± 0.2	-52870 ± 200
CL-P5	8.09	55.0 ± 0.1	-53110 ± 200

[a] The energies in this row are averaged over the simulation period 20–70 ps for the CA-P2 model since the ion exited from the channel after 70 ps (see Fig. 6)

These data clearly indicate that the surface areas of the different systems are distributed over a narrow region (from 7.87 to 8.17 nm^2). Furthermore, the standard deviations of volumes and potential energies are all very small compared with their average values (below 0.4%). Therefore, all these data demonstrate that the systems were equilibrated and our construction method was valid.

Dynamic properties of ions and water molecules in the pore region

In this section, some dynamic properties of ions in the channel pore region were explored by analyzing the MD trajectories of ions. The long axis of the GA channel was set to parallel to the *Z*-axis of the model system (the normal direction of bilayer) so that the *Z*-coordinate change of the ion with simulation time could help us visualize the translocation of ions in the pore region. Since the peptide backbone of GA did not make significant fluctuation for the ion and water in the channel pore along the *Z*-axis during all the simulations, the *Z*-coordinate change could represent the real motion of the ion and the pore water molecule along the channel axis. Moreover, since all the GA-DMPC systems with ions were initially equilibrated enough at each chosen position, the system had sufficient time to respond to the presence of the ion. Figure 3 shows the *Z*-coordinate change of different ions with simulation time for the 15 model systems. It is clear that the motions of Na^+ and Ca^{2+} ions were provided with small fluctuations within the 100 ps simulation period (see Fig. 3a and b). For the Cl^- ion, its dramatic change in position for the CL-P2 and CL-P3 models (see Fig. 3c) indicates an unfavorable environment for the Cl^- ion in the pore region of the GA channel. These results may explain why Na^+ and Ca^{2+} ions can enter the pore region of the channel while the Cl^- ion cannot (Andersen 1984; Wallace 1990). On the other hand, compared to the CL-P2 and CL-P3 models, the ions in the CL-P4 and CL-P5 models are fairly stable during the simulations. One possible explanation is that there could be a local energy minimum near the center of the GA channel for Cl^-, while a large energy barrier near the entrance of the channel has been proposed in previous work (Roux and Karplus 1994). In addition, although most trajectories of the Na^+ and Ca^{2+} ions are fairly stable during MD simulations, there are some obvious movements of ions, such as the point E marked in Fig. 3b. Such a change may indicate a process where the Ca^{2+} ion exited from the pore region of the channel to the bulk solvent. Movement of water molecules beside the ion was involved in this process, which will be discussed in detail later.

It is well known that pore water is an important issue in the ion permeation of the channel. Because the motion of pore water is dominant in one dimension (long axis of the channel pore) and the interaction between ion and water is very strong, the conformational and dynamic properties of pore water show different characteristics from bulk water. Figure 4 shows three snapshots of GA configuration for different models with water and ions in the pore regions. The dipole orientations of water molecules for different models changed according to the positions and types of ion. For the GD-H2O model, the dipoles of the water molecules in the pore region were almost parallel to each other, and all the water molecules were connected to each other by a H-bond network to form a water chain. However, this chain was broken by the existence of ions, and the dipoles of the water molecules were all re-orientated by the ion. For the CA-P5 model, the Ca^{2+} ion caused the dipole of pore water to point to bulk solvent. However, in the case of the CL-P5 model, the Cl^- ion forced the dipole of pore water to point toward itself. This result is in agreement with

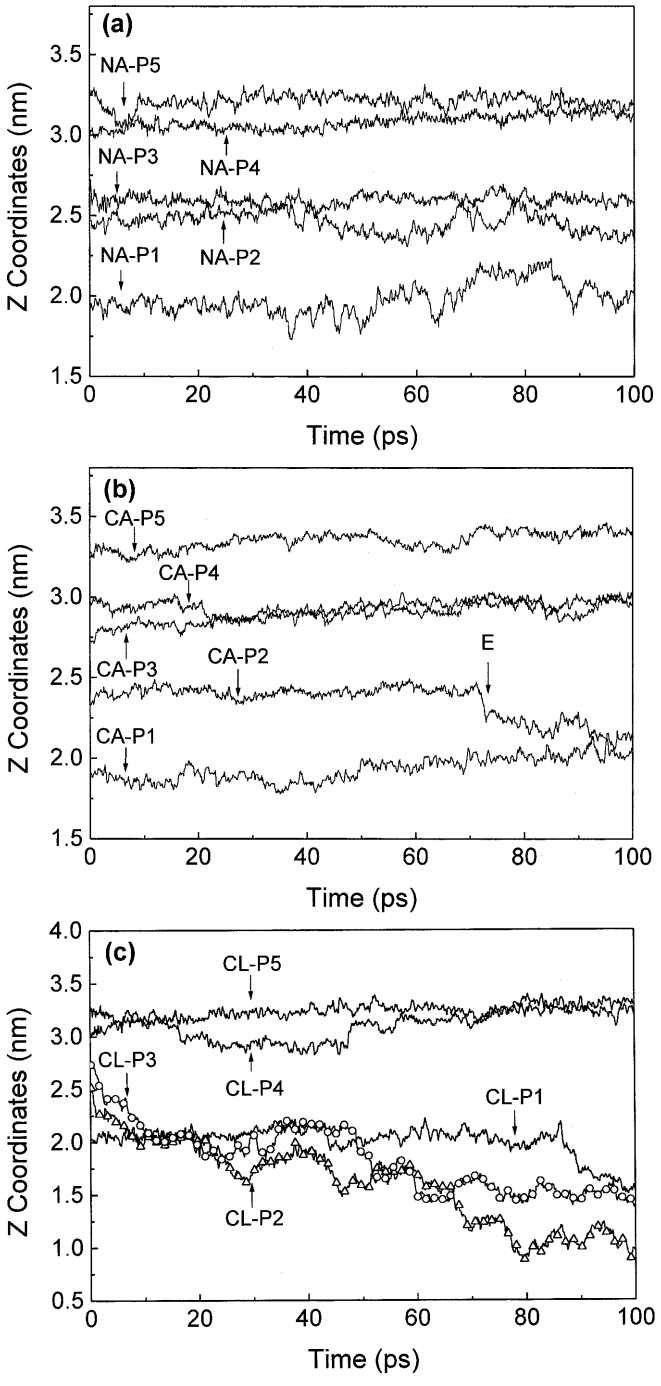

Fig. 3 *Z*-coordinates of different ions in all 15 models as a function of the simulation time: **a** for the Na^+ ion; **b** for the Ca^{2+} ion; **c** for the Cl^- ion. The E position in **b** displays an exiting process of the Ca^{2+} ion from the pore region to the bulk solvent. In order to show the exit process of the Cl^- ion, all the 100 ps simulation, including the first 50 ps equilibration process, is shown in this figure

previous studies on the properties of water in the ion channel (Roux and Karplus 1994). The reorientation of the water dipole is very important for hydration of the ion in the pore region and to lower the energy barrier for ion permeation because it provides solvation energy for the ion in the pore region.

Since the motion of the pore water molecules is mainly constricted in one dimension, the change in *Z*-coordinates of pore waters with the simulation time can display their dynamic behavior. The *Z*-coordinates of the oxygen atoms of the pore waters are used to represent the water molecules. Figure 5 displays motions of both the pore water molecules and the Ca^{2+} ion for two different models. For the GD-H2O model, the motions of pore water molecules are strongly coupled to each other by the H-bond network. However, it should be noticed that there are some differences for water motions at the positions marked A and P in Fig. 5a. The distance between the water positions had a large change at position A (W140 and W205). This suggests that there are some flip-flops of water molecules in the channel. The same result has been shown in previous MD simulations by Chiu and co-workers (1999b). These flip-flops of the water dipole may play a significant role in the movement of water molecules and further affect the translocation of ions in the channel pore region, since the ion permeation process is actually translocation of the center of mass of the ion and the pore waters. On the other hand, comparison between Fig. 5a and b shows the different dynamic properties of the pore water molecules for both models. As shown in Fig. 5b, it is obvious that the motions of the two water molecules (W140 and W231) beside the Ca^{2+} ion are strongly coupled with that of the ion owing to the strong interaction between them. However, the motion of other water molecules (W150 and W195) is somewhat less coupled with the ion's movement. In other words, the long-distance coupling of water motions is broken owing to the presence of the ion, while this feature is more dominant for the pore water molecules in the case of the model without the ion.

To show the exiting process of the Ca^{2+} ion in the simulation of the CA-P2 model, the trajectories of the Ca^{2+} ion and its nearby water molecules are displayed in Fig. 6. The similarity between the trajectory of the ion and its two nearby water molecules (W110 and W195) indicated that the exiting process of the Ca^{2+} ion was coupled with these two water molecules. However, the obvious difference in the trajectory after 70 ps shows that the coupling between them was broken when they entered into bulk solvent. On the other hand, one of the bulk waters (W178) entered into the pore region during this process and filled the vacancy caused by the ion's exit. This result suggests that the ion exiting process involved strongly binding waters of the ion. Therefore, the above process provides an insight into the rehydration process of the ion from the pore region to the bulk solvent, which is a key step in the ion permeation process.

Structural properties of the GA channel

In the preceding section, we analyzed the trajectories of the ions and the pore water molecules to help us gain

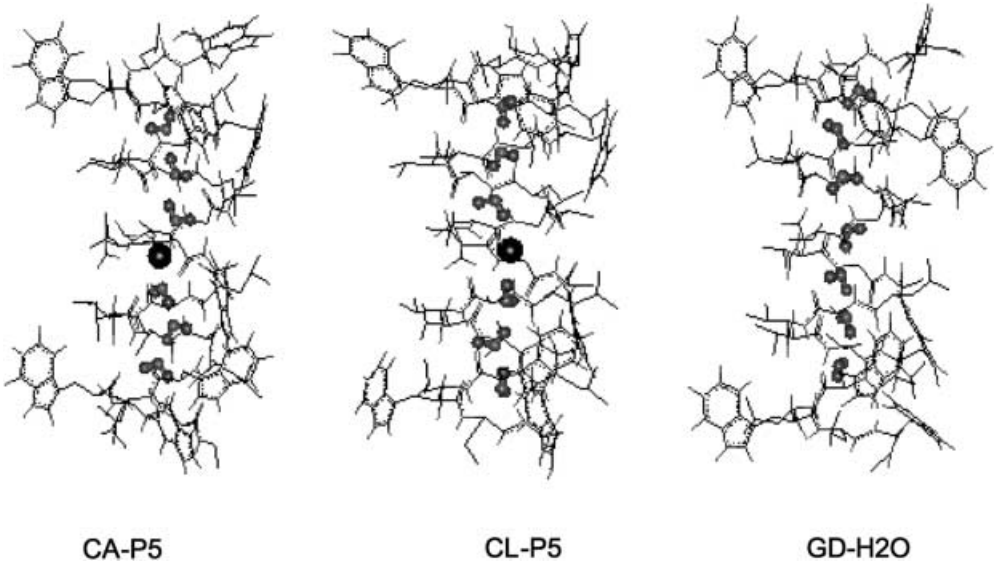

Fig. 4 View of the orientation of water dipoles in three different models: the GD-H2O model, the CA-P5 model, and the CL-P5 model. The ions Ca^{2+} and Cl^{-} are shown as *dark circles*

some insight into the motion of ion and water in the channel pore region. In this section, we focus on structural properties of the GA channel with an ion in the pore. In order to reveal how the ion affects the conformation of GA, the GA configurations from simulations for different models were analyzed and compared with each other.

The pore radius of an ion channel is an important factor in determining the selectivity of ions and the energy barrier for ion permeation. In previous modeling and theoretical calculations of the GA channel, the backbone atoms of the GA channel are often constrained to simplify the simulation and save computation time, so that the channel pore radius is constant in these studies (Roux and Karplus 1994). However, many recent studies have demonstrated that the flexibility of GA, especially the backbone atoms of GA, is very important for the motion of the ion and the pore waters (Chiu et al. 1989). Since no restraint was used in the present study, we were able to use pore radius as an index to determine changes in the structure of GA caused by the ion. Figure 7 shows the pore radius of the

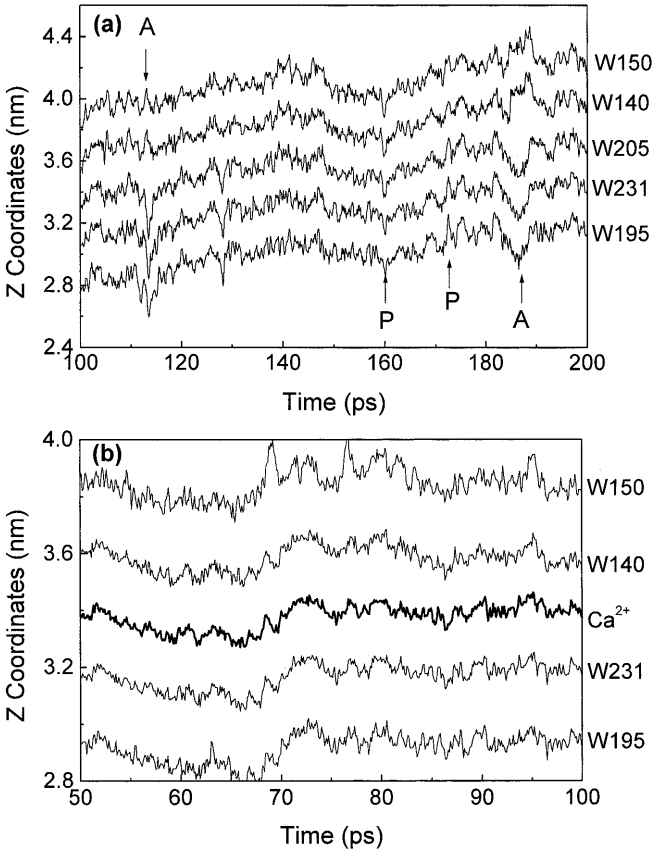

Fig. 5 *Z*-coordinates of the pore water molecules for two different models after the equilibration process: **a** the GD-H2O model (100–200 ps); **b** the CA-P5 model (50–100 ps). The *dark line* in **b** is for the trajectory of the Ca^{2+} ion

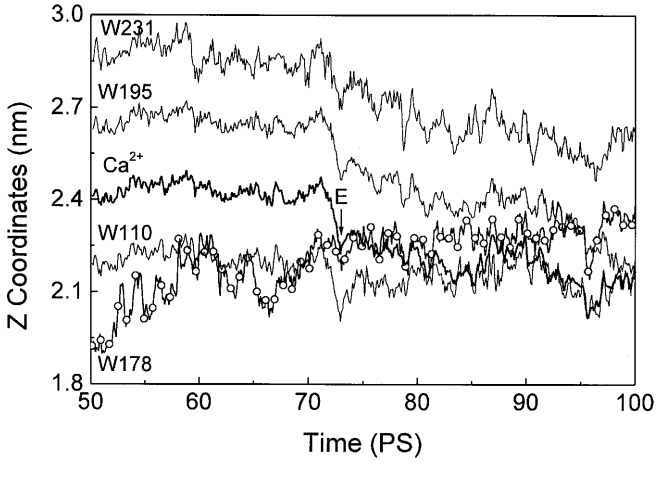

Fig. 6 *Z*-coordinate trajectory of the Ca^{2+} ion and pore water molecules. The exiting process of the Ca^{2+} ion from the pore region to the bulk solvent was extracted from the CA-P2 model. The trajectory of the Ca^{2+} ion is plotted with a *dark line* and the water molecule W178 entering into the pore region is plotted as ○

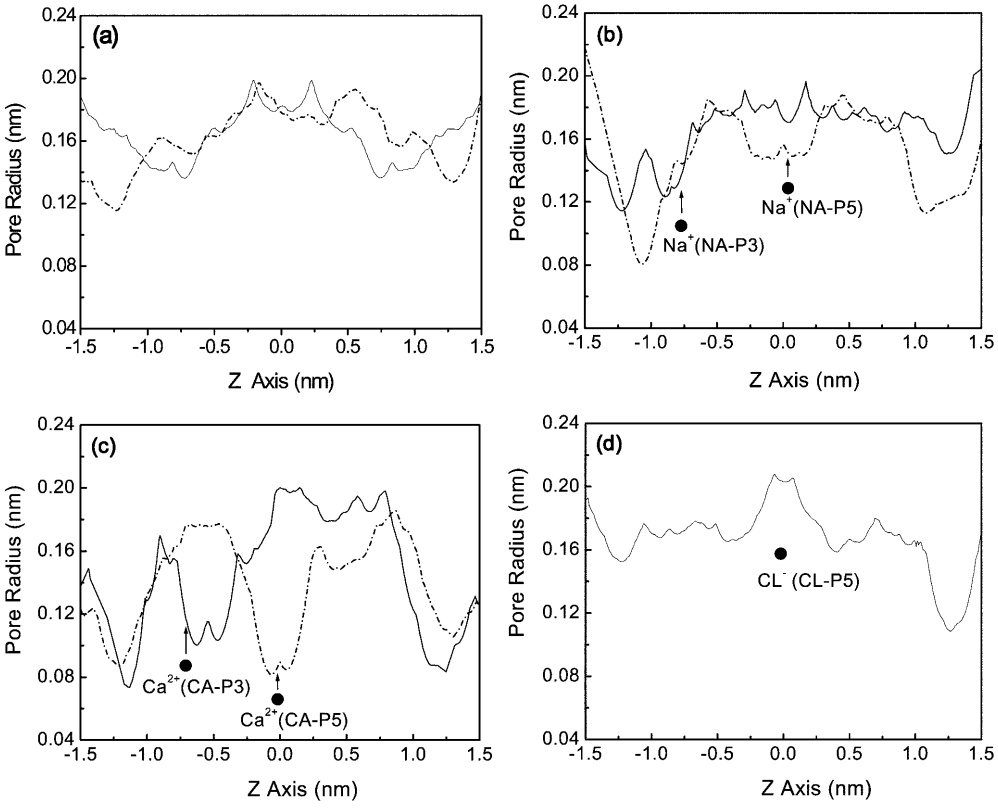

Fig. 7 The pore radius of the GA channel along the channel axis for different models: **a** the 1MAG model (*solid line*) and the GD-H2O model (*dashed line*); **b** the NA-P3 model (*solid line*) and the NA-P5 model (*dashed line*); **c** the CA-P3 model (*solid line*) and the CA-P5 model (*dashed line*); **d** the CL-P5 model (*solid line*). The *filled circles* show the positions of the ions Na^+, Ca^{2+}, and Cl^- in the different models

GA channel as a function of position along the channel axis in different model systems. Since positions P1 and P2 were outside the entrance of the pore region and the Cl^- ion in the CL-P3 model was pushed back from the channel pore region, only six models (CA-P3, CA-P5, NA-P3, NA-P5, CL-P5, and GD-H2O model) are chosen to measure the pore radius. In addition, the pore radius of the GA channel, obtained from NMR experiments (1MAG) (Ketchem et al. 1993), was also calculated and used as a reference for comparison in Fig. 7a.

From Fig. 7, it is obvious that the influence of the ion on the pore radius is dependent on its electrical properties and charge. For instance, the Ca^{2+} and Na^+ ions are cations that should reduce the local pore radius, while the Cl^- ion is an anion that would enlarge the local pore radius. For the GD-H2O model, the pore radius has no predominant regular changes compared with the 1MAG model (see Fig. 7a). As shown in Fig. 7b–d, it is evident that the change in pore radius caused by the Ca^{2+} ion is bigger than that caused by the Na^+ or Cl^- ion. Using the pore radius of the 1MAG model as reference, the local pore radius of the GA channel reduced 0.01 nm for the NA-P3 model and 0.03 nm for the NA-P5 model, while this value reduced 0.03 nm in the CA-P3 model and 0.09 nm in the CA-P5 model. The stronger attractive interaction between the Ca^{2+} ion and the backbone atoms of the GA channel was responsible for the bigger change in the local pore radius. From Fig. 7 it is also found that the ion has a local effect on the channel pore radius, and only pore radii beside the ion position have obvious changes. This result was supported by NMR studies on the effect of Na^+ ions on the GA channel at its binding site (Smith et al. 1990; Cross and Opella 1994). On the other hand, in the CL-P5 model the local pore radius increased 0.03 nm (see Fig. 7d) owing to the repulsive interaction between the Cl^- ion and the GA carbonyl oxygen.

In addition, other than the ion-GA interaction, another important factor, the ionic radius, should be taken into consideration in explaining the above results. The radii of Na^+, Ca^{2+}, and Cl^- ions in the ionic crystal state are 0.095, 0.099, and 0.181 nm, respectively (Dean 1979). Therefore, for the case of the Ca^{2+} ion, the local pore radius near the ion position was similar to the ion radius: 0.11 nm in the CA-P3 model and 0.09 nm in the CA-P5 model. This indicates that the Ca^{2+} ion has close contact with the backbone atoms and explains why Ca^{2+} ions can block the GA channel based on the ion radius. For the Na^+ and Cl^- ions, the local pore radii near the ion position (0.13 nm in the NA-P3 model, 0.15 nm in the NA-P5 model, and 0.21 nm in the CL-P5 model) are all significantly larger than their ionic radii. This shows a weaker interaction between these ions and the GA channel. On the other hand, this leads to less deformation of the backbone atoms. It is well known that the GA channel is permeable for monovalent cations with the selectivity tendency $Li^+ < Na^+ < K^+ < Rb^+ < Cs^+$ (Andersen 1984; Wallace 1990), but it is still unclear what factors determine this phenomenon. Based on the above analysis of the relation between an ion and the local pore radius, we are able to propose a reasonable mechanism for this selec-

tivity. From Fig. 7a it was found that most pore radii are between 0.16 and 0.18 nm for the 1MAG and GD-H2O models. However, the ionic radii of monovalent cations in the crystal state are 0.084 nm for Li^+, 0.095 nm for Na^+, 0.133 nm for K^+, 0.148 nm for Rb^+, and 0.169 nm for Cs^+ (Dean 1979). The Cs^+ ion radius is matched best to the pore radius of GA while the Li^+ ion matches worst and may cause more changes to the pore radius and distortion of the channel backbone. Moreover, the dehydration energy of a small size ion (such as Li^+) is bigger than that of a large size ion (such as Cs^+). For the case of the Li^+ ion, more energy is required to remove water and to attract the channel carbonyl oxygen more strongly compared to the Cs^+ ion. This causes more distortion of the GA channel. Since greater distortion of the GA channel means a more unfavorable state, this can increase the free energy of ion permeation, and thus the Cs^+ ion with a large ionic radius permeates the GA channel easier than the Li^+ ion. In addition, a popular view is that the smallest radius in the pore region is the key factor to determine whether the ion can pass through the channel, but this is now questionable since from the above result the local radius can be changed by the ion. We suggest that the smallest radius will play a significant role in ion selectivity only when located in a less flexible region. In the case of the GA channel, it is unlikely that the smallest pore radius determines ion selectivity because it is located near the entrance of the GA channel, a very flexible region.

Another interesting result was that the pore radii at the two ends of the pore region for the various models were very different. Through analysis of the trajectories and visualization of GA conformations, it was found that the flexible conformation of the ethanolamine group was the main reason for this result. Figure 8 displays three conformations of the channel entrance for different models with their corresponding profiles of the pore radius. The ethanolamine group is emphasized using the ball-stick representation. From this figure it is clear that the ethanolamine group has a dominant influence on the pore radius at the entrance of the GA channel. When the ethanolamine group swung far from the center of the channel pore (see Fig. 8a), the local pore radius was much bigger (see Fig. 8b). However, when the group swung into the central region of the channel pore, such as for the CA-P3 model in Fig. 8a, the corresponding local pore radius was much smaller than the normal pore radius. This means the ethanolamine group may play a key role in determining the local pore radius at the entrance of the channel. In addition, theoretical calculations of the energy profile in the GA channel by Etchebest et al. (1985) showed that the flexibility of the ethanolamine group modified the profile considerably. We suggest that this swinging motion of the ethanolamine group is very important to ion permeation since the dehydration process of the ion takes place in the region, and this type of motion may be relevant to the dehydration and re-hydration processes.

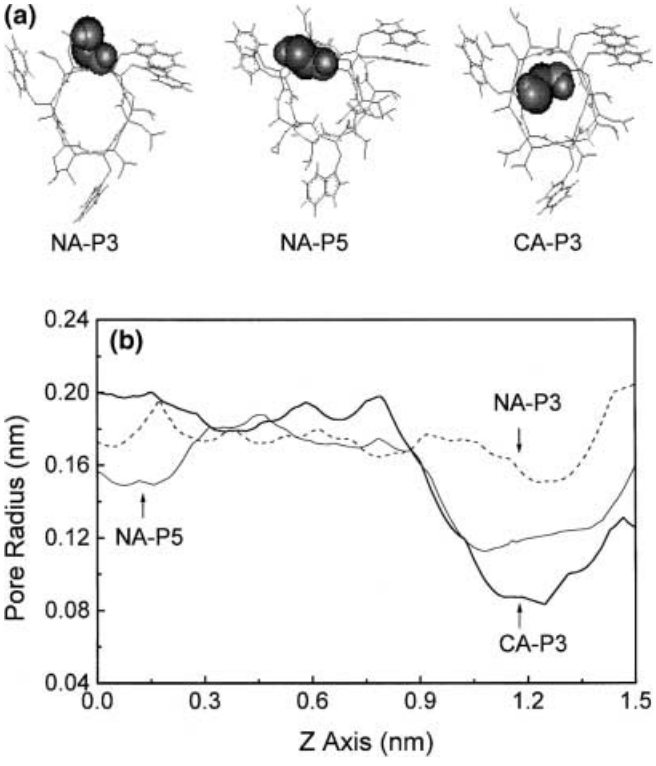

Fig. 8a, b Influence of the conformation of the ethanolamine group on pore radius at the entrance of the GA channel. **a** View of the GA conformation for three models: NA-P3, NA-P5, and CA-P3 along the channel axis; the ethanolamine group is displayed in *space-filled style*. **b** The pore radius profiles for the same three models shown in **a**

As discussed above, the ion had a significant effect on the local pore radius of the GA channel. What causes this result? Comparing the GA configuration obtained from MD simulation with that of the 1MAG model, it is possible to shed light on the reason for these changes. Figure 9 shows the root-mean-square deviation (r.m.s.d.) of the C and O atoms of the C=O group in GA from three different models (the GD-H2O, the NA-P3, and the CA-P3) relative to that of the 1MAG model. From Fig. 9a it is clear that the GA structure in the GD-H2O model system was most consistent with that of the 1MAG model, especially in the central region of the GA monomer. However, as to the GA configuration for both the NA-P3 and the CA-P3 model systems, the r.m.s.d. values of the C and O atoms near the central region of the GA monomer (where the ion resides) showed obvious changes. This suggests that both the C and O atoms play important roles for changing the local pore radius around the ion position. Moreover, it is obvious that the Ca^{2+} ion causes more change in the r.m.s.d. than Na^+. This result is consistent with the local pore radius changes as discussed above. From Fig. 9, the following two reasons can be given for the change in local pore radius. One is a distortion in helix backbone since there was a significant change in the r.m.s.d. for C atoms. The other is reorientation of the C=O bond. As shown in Fig. 9b and c, it was found that the r.m.s.d. for

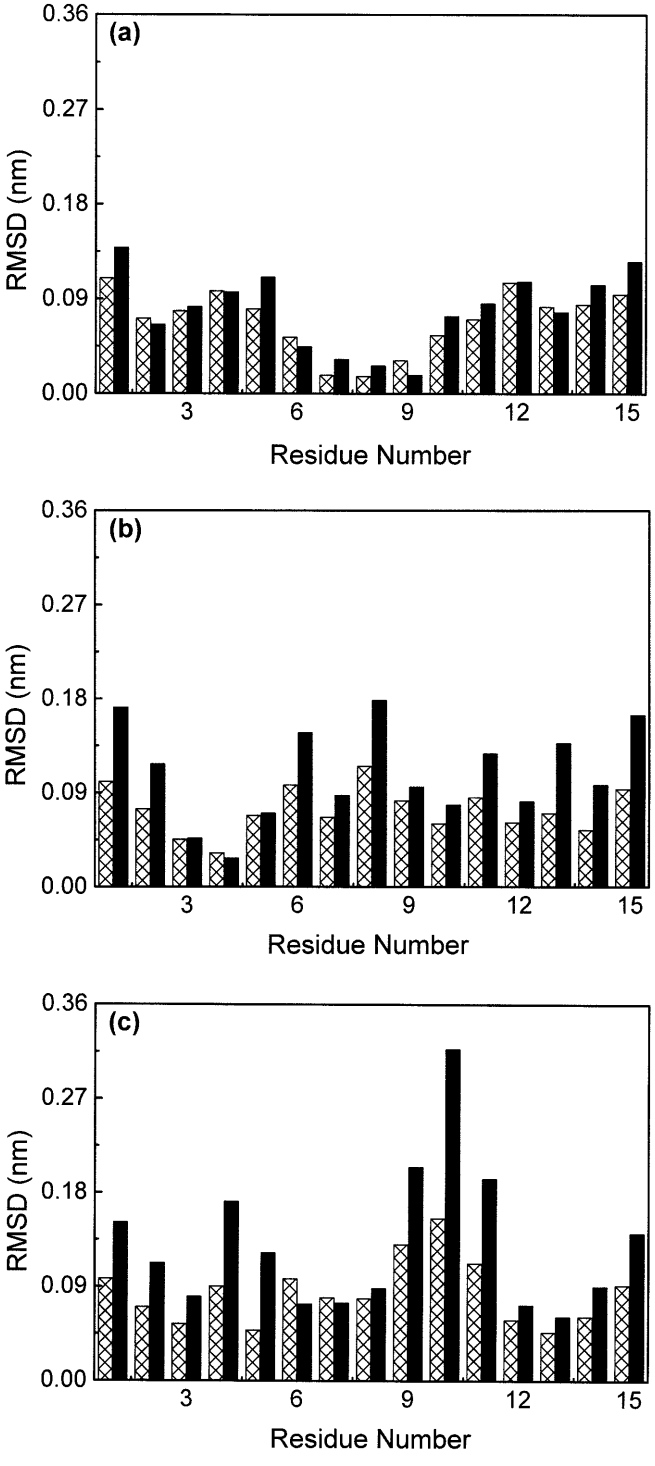

Fig. 9 R.m.s.d. of the C and O atoms of the C=O groups in the GA backbone relative to the experimental structure (1MAG) for three different models: **a** the GD-H2O model; **b** the NA-P3 model; **c** the CA-P3 model. The *black bars* are for the O atom and the others for the C atom

O atoms are generally larger than for C atoms near the ion. Since the C=O bond length was fixed with the SHAKE constraint algorithm during the MD simulations, only reorientation of the C=O bond could lead to the above result. Another interesting feature is an alternating increase in the r.m.s.d. values for O atoms in Fig. 9b (residues 6 and 8) and Fig. 9c (residues 9 and 11). This could be related to the property of the GA helix consisting of alternating L- and D-forms of amino acids. However, residue 10 in Fig. 9c showed a dramatic increase for the r.m.s.d. value of the O atom (more than 0.3 nm), which was caused by a rotation of the C=O bond of approximately 180°. In fact, it is unreasonable for backbone atoms of GA to make such a large and destructive deformation; thus there should be other kinds of mechanism taken by divalent cations in the channel. An NMR study of Mn^{2+} ion in binding sites of GA by Golovanov et al. (1991) showed that the Mn^{2+} ion retained its hydrate shell in the channel. Our result demonstrates a strong influence of the Ca^{2+} ion on the conformation of the GA channel, similar to the Mn^{2+} ion in the GA channel. In addition, the r.m.s.d. values of the C and O atoms for residues at the two ends of the helix are generally larger than that in the central region, except for those affected by the ion. This indicates that residues near the two ends of the helix were more flexible than those located in the central region of the GA monomer, which reinforces the conclusion based on the analysis of the conformation of the ethanolamine group earlier.

Table 2 Interaction energies between the ion and other components (water, GA, and DMPC)[a]

System	Ion-water	Ion-GA	Ion-DMPC	Total
NA-P1	–546 ± 82	–19 ± 15	–126 ± 62	–691
NA-P2	–271 ± 61	–305 ± 55	5 ± 48	–571
NA-P3	–269 ± 37	–290 ± 38	4 ± 16	–545
NA-P4	–284 ± 25	–250 ± 47	–5 ± 20	–529
NA-P5	–287 ± 24	–262 ± 46	–3 ± 7	–552
CA-P1	–2053 ± 116	–59 ± 30	–304 ± 70	–2416
CA-P2[b]	–750 ± 82	–902 ± 52	–94 ± 44	–1756
CA-P3	–487 ± 53	–1097 ± 52	–72 ± 48	–1656
CA-P4	–475 ± 68	–1082 ± 65	–82 ± 32	–1639
CA-P5	–507 ± 37	–1039 ± 54	–6 ± 7	–1552
CL-P1[c]	–411 ± 74	–17 ± 28	–119 ± 69	–537
CL-P5[c]	–151 ± 22	–152 ± 34	–1 ± 14	–303

[a] The unit of interaction energies is kJ/mol. The standard deviations are also displayed in the table, except for the total energies

[b] The energies in this row are averaged over the simulation period 20–70 ps for the CA-P2 model for the same reason explained in Table 1

[c] Since the Cl^- ion in the CL-P2 and CL-P3 models exited from the channel and the trajectory of the CL-P4 model was similar to that of the CL-P5 model, the data for the CL-P2, CL-P3, and CL-P4 models are excluded from this table (see Fig. 3c)

Interaction energies between main components

Table 2 reports interaction energies between the ion and other components for the different model systems. From the table, the following points can be extracted:

1. All ions lost much interaction energy with water molecules when they entered into the pore region of the GA channel (see the second column of Table 2).

However, as shown in the third column of the table, the loss of this absolute interaction energy was mostly compensated by the increase in absolute interaction energy between the ion and the GA channel.

2. From the fourth column, the DMPC lipids had a significant effect on the entrance process of the ion into the pore region. When the ion was near the entrance of the GA channel (P1 models), the interaction energy (mainly the electrostatic interaction) between the ion and the head-groups was more negative. However, when the ion enters into the pore region, the distance between the ion and the head-groups of the DMPC lipids increases so much that both electrostatic and van der Waals interactions between the ion and the DMPC lipids decreased rapidly in the pore region. For instance, the interaction energy between the ion and DMPC is about –125 kJ/mol in the NA-P1 model and only –3 kJ/mol in the NA-P5 model. This implies that the influence of the lipid on ion permeation is mainly restricted to the entrance of the channel, which prevents the ion entering into the pore region. A similar result was proposed in previous MD simulations of the GA-DMPC system (Chiu et al. 1999a), in which it was found that the head-groups of DMPC lipids obstructed the water molecules in the pore region.
3. The total interaction energy between the Na^+ ion and other components in the NA-P1 and the NA-P5 systems was more negative than for the CL-P1 and the CL-P5 models, respectively. This may explain why the Cl^- ion could not permeate the GA channel from the viewpoint of the interaction energy.

Table 3 lists interaction energies between GA and other components in the model systems. As shown in this table, all the interaction energies between GA and DMPC lipids for the different models were similar. This suggests that the GA-DMPC interaction is little affected by the existence of ions in the pore region.

Table 3 Interaction energies between GA and other components (GA, water, and DMPC) for different systems[a]

System	GA-GA	GA-water	GA-DMPC
NA-P1	–1340 ± 42	–581 ± 72	–1227 ± 44
NA-P2	–1275 ± 44	–448 ± 57	–1190 ± 40
NA-P3	–1251 ± 43	–461 ± 65	–1212 ± 43
NA-P4	–1264 ± 44	–502 ± 67	–1172 ± 45
NA-P5	–1279 ± 47	–524 ± 60	–1156 ± 42
CA-P1	–1323 ± 46	–558 ± 64	–1203 ± 45
CA-P2[b]	–1157 ± 48	–430 ± 63	–1140 ± 53
CA-P3	–976 ± 52	–403 ± 58	–1179 ± 54
CA-P4	–953 ± 54	–393 ± 60	–1201 ± 52
CA-P5	–1051 ± 58	–432 ± 63	–1199 ± 57
CL-P1[c]	–1379 ± 48	–583 ± 62	–1186 ± 44
CL-P5[c]	–1303 ± 47	–503 ± 60	–1162 ± 47

[a] See footnote [a] to Table 2
[b] See footnote [b] to Table 2
[c] See footnote [c] to Table 2

Conclusions

In this paper, we present a systematic study of the interactions between ions and the GA channel during the ion permeation process. The initial configuration of the GA-DMPC model was constructed using our previous method (Tang et al. 1999). Three different ions (Na^+, Ca^{2+}, and Cl^-) were added to one of five different positions in the pore region by replacing one of the pore water molecules. A 100 ps MD simulation was performed for each model. Since no restraints were added in the simulations, the results of the simulations may give us more realistic descriptions of the interaction between the ion and the GA channel during the ion permeation process. The GROMOS 96 software package was used for this study, and the results show that the package is well established for the simulation of proteins in a lipid environment.

It was shown that Na^+ and Ca^{2+} ions could fluctuate stably in the pore region. However, Cl^- ions (especially at P2 and P3 position) were pushed quickly back from the pore region during the starting 50 ps MD simulation because of unfavorable interactions between the ion and the GA channel. This result is consistent with experimental data for the GA channel. In addition, it was found that the flexibility of the GA channel is an important factor for the ion permeation process. The local pore radius of the GA channel near the ion position changed according to the ion charge, number of charges, and ion radius. The Cl^- ion was able to enlarge the local pore radius and both Na^+ and Ca^{2+} ions were able to reduce the local pore radius. Furthermore, the local pore radius was changed more by the Ca^{2+} ion than the Na^+ ion because of its higher charge quantity. This result helps us explain the greater stability of the Ca^{2+} ion in the pore region and the blocking of the GA channel. This suggests that both the ion and the channel have significant influence on one another during ion permeation. The GA channel provides solvation energy for the ion, which favors the translocation of the ion in the channel pore region. On the other hand, ion permeation causes a conformational change in GA, the main change being in the local pore radius due to the distortion of the backbone and reorientation of the C=O dipole in the GA.

Through analysis of the interaction energy and GA conformation of the different models, it was found that the ethanolamine group of GA and the DMPC lipids play important roles in the regulation of ion entry into the GA pore region. The ethanolamine groups were very flexible and moved into the entrance region of the channel to block the pore region. This suggests that the ethanolamine group can be seen as a gate, which might be responsible for channel gating. DMPC lipids also had an effect on the entrance process of the ion, owing to strong interactions with ions in this region.

Water molecules in the channel were also indispensable parts of the ion permeation process. The ion had a

distinct influence on the structural and dynamic properties of the pore water molecules. With the ion present in the pore region, the dipoles of water molecules were reoriented, depending on ion position and charge. Two pore water molecules adjacent to the ion were strongly coupled to the ion, but less correlation with the ion was found for other pore water molecules in the second or higher shell. Moreover, when the ion exited from the pore region, the coupled pore waters also exited the pore region. Meanwhile, bulk water could enter into the pore region to fill the space vacancy caused by the ion leaving.

Although the MD simulation time in the present study was somewhat smaller compared to the realistic ion permeation process, some understanding of ion-channel interactions during channel permeation can be obtained from this study. This can help us propose possible mechanisms for the ion permeation process and promote a more realistic description and accurate understanding of this important process. Further study of other channel systems and longer MD simulations will be required.

Acknowledgements We thank Prof. van Gunsteren for kindly providing us with the GROMOS 96 package and Dr. Marrink for kindly sending us the equilibrium configurations of DMPC lipids. We also thank Prof. Jakobsson, Dr. Cheng, and Dr. Chiu for helpful discussions. This work was supported in part by the Chinese National Natural Science Foundation (nos. 29992590-2, 39670187, and 19774501) and the Beijing Natural Science Foundation (no. 5992002).

References

Andersen OS (1984) Gramicidin channels. Annu Rev Physiol 46: 531–548

Berendsen HJC, Postma JPM, Gunsteren WF van, Dinola A, Haak JR (1984) Molecular dynamics with coupling to an external bath. J Chem Phys 81: 3684–3690

Berendsen HJC, Grigera JR, Straatsma TP (1987) The missing term in effective pair potentials. J Phys Chem 91: 6269–6271

Berger O, Edholm O, Jahnig F (1997) Molecular dynamics simulations of a fluid bilayer of dipalmitoylphosphatidylcholine at full hydration, constant pressure, and constant temperature. Biophys J 72: 2002–2013

Cheng W, Wang CX, Chen WZ, Xu YW, Shi YY (1998) Investigating the dielectric effects of channel pore water on the electrostatic barriers of the permeation ion by the finite difference Poission-Boltzmann method. Eur Biophys J 27: 105–112

Chiu SW, Subramaniam S, Jakobsson E, MaCammon JA (1989) Water and polypeptide conformation in the gramicidin channel. Biophys J 56: 253–261

Chiu SW, Subramaniam S, Jakobsson E (1999a) Simulation study of a gramicidin/lipid bilayer system in excess water and lipid. I. Structure of the molecular complex. Biophys J 76: 1929–1938

Chiu SW, Subramaniam S, Jakobsson E (1999b) Simulation study of a gramicidin/lipid bilayer system in excess water and lipid. II. Rates and mechanisms of water transport. Biophys J 76: 1939–1950

Cross TA, Opella SJ (1994) Solid-state NMR structural studies of peptides and proteins in membranes. Curr Opin Struct Biol 4: 547–581

Dean AJ (1979) Handbook of chemistry. McGraw-Hill, New York

Egberts E, Berendsen HJC (1988) Molecular dynamics simulation of a smectic liquid crystal with atomic detail. J Chem Phys 89: 3718–3732

Egberts E, Marrink SJ, Berendsen HJC (1994) Molecular dynamics simulation of a phospholipid membrane. Eur Biophys J 22: 423–436

Etchebest C, Pullman A, Ranganathan S (1985) The gramicidin A channel: theoretical energy profile computed for single occupancy by a divalent cation calcium. Biochim Biophys Acta 818: 23–30

Fischer W, Brickmann J, Lauger P (1981) Molecular dynamics study of ion transport in transmembrane protein channels. Biophys Chem 13: 105–116

Fornili SL, Vercauteren DP, Clementi E (1984) Water structure in the gramicidin A transmembrane channel. Biochim Biophys Acta 771: 151–164

Golovanov AP, Barsukov IL, Arseniev AS, Bystrov VF, Sukhanov SV, Barsukov LI (1991) The divalent cation-binding sites of gramicidin A transmembrane ion-channel. Biopolymers 31: 425–434

Gunsteren WF van, Berendsen HJC (1977) Algorithms for macromolecular dynamics and constraint dynamics. Mol Phys 34: 1311–1327

Gunsteren WF van, Billeter SR, Eising AA, Hünenberger PH, Krüger P, Mark AE, Scott WRP, Tironi IG (1996) Biomolecular simulation: the GROMOS 96 manual and user guide. Vdf Hochschuverlag an der ETH Zürich, Zurich, Switzerland

Heller H, Schaefer M, Schulten K (1993) Molecular dynamics simulation of a bilayer of 200 lipid in the gel and in the liquid-crystal phases. J Phys Chem 97: 8343–8360

Hunenberger PH, Gunsteren WF van (1998) Alternative schemes for the inclusion of a reaction-field correction into molecular dynamics simulations: influence on the simulated energetic, structural, and dielectric properties of liquid water. J Chem Phys 108: 6117–6134

Jakobsson E (1997) Computer simulation studies of biological membranes: progress, promise and pitfalls. Trends Biochem Sci 22: 339–344

Ketchem RR, Hu W, Cross TA (1993) High-resolution conformation of gramicidin A in a lipid bilayer by solid-state NMR. Science 261: 1457–1460

Koeppe RE II, Andersen OS (1996) Engineering the gramicidin channel. Annu Rev Biophys Biomol Struct 25: 231–258

Kirkpatrick S, Gelatt CD Jr, Vecchi MP (1983) Optimization by simulated annealing. Science 220: 671–679

Latorre R (ed) (1986) Ionic channels in cells and model systems. Plenum Press, New York

Mackay DH, Berens PH, Wilson KR, Hagler AT (1984) Structure and dynamics of ion transport through gramicidin A. Biophys J 46: 229–248

Merz KM Jr (1997) Molecular dynamics simulation of lipid bilayer. Curr Opin Struct Biol 7: 511–517

Montal M (1996) Protein folds in channel structure. Curr Opin Struct Biol 6: 499–510

Pastor RW (1994) Molecular dynamics and Monte Carlo simulation of lipid bilayer. Curr Opin Struct Biol 4: 486–492

Pastor RW, Venable RM, Karplus M (1991) Model for the structure of the lipid bilayer. Proc Natl Acad Sci USA 88: 892–896

Pullman A (1985) Computed energy profiles for ion transport in the gramicidin A channel. J Biosci 8: 1–2

Roux B, Karplus M (1988) The normal modes of the gramicidin A dimer channel. Biophys J 53: 297–309

Roux B, Karplus M (1994) Molecular dynamics simulation of the gramicidin channel. Annu Rev Biophys Biomol Struct 23: 731–761

Ryckaert JP, Bellemans A (1975) Molecular dynamics of liquid n-butane near boiling point. Chem Phys Lett 30: 123–125

Ryckaert JP, Ciccotti G, Berendsen HJC (1977) Numerical integration of the Cartesian equations of motion of a system with constraints: molecular dynamics of n-alkanes. J Comput Phys 23: 327–341

Sayle RA, Millner-White EJ (1995) Rasmol biomolecular graphics for all. Trends Biochem Sci 20: 374–376

Smart OS, Goodfellow JM, Wallace BA (1993) The pore dimensions of gramicidin A. Biophys J 65: 2455–2460

Smith R, Thomas DE, Atkins AR, Separovic F, Cornell BA (1990) Solid-state carbon-13 NMR studies of the effects of sodium ions on the gramicidin A ion channel. Biochim Biophys Acta 1026: 161–166

Tang YZ, Chen WZ, Wang CX, Shi YY (1999) Constructing the suitable initial configuration of the membrane-protein system in MD simulations. Eur Biophys J 28: 478–488

Tieleman DP, Berendsen HJC (1996) Molecular dynamics simulation of a fully hydrated dipalmitoylphosphatidylcholine bilayer with different macroscopic boundary conditions and parameters. J Chem Phys 105: 4871–3880

Wallace BA (1990) Gramicidin channels and pores. Annu Rev Biophys Chem 19: 127–157

Woolf TB, Roux B (1994) Molecular dynamics simulation of the gramicidin channel in a phospholipid bilayer. Proc Natl Acad Sci USA 91: 11631–11635

Woolf TB, Roux B (1996) Structure, energetic, and dynamics of lipid-protein interaction: a molecular dynamics study of the gramicidin A channel in a DMPC bilayer. Proteins Struct Funct Genet 24: 92–114

Woolf TB, Roux B (1997) The binding site of sodium in the gramicidin A channel: comparison of molecular dynamics with solid-state NMR data. Biophys J 72: 1930–1945